Supporting Information 1 for

Enhancements of Loading Capacity and Moving Ability by Microstructures for Wireless Soft Robot Boat

Tian Li, Weitao Jiang*, Jie Han, Dong Niu, Hongzhong Liu, Bingheng Lu

State Key Laboratory for Manufacturing Systems Engineering, Xi'an Jiaotong University, Xi'an 710049, China.

E-mail: wtjiang@mail.xjtu.edu.cn

No. of figures: 3

No. of Tables: 1

No. of Equations: 7

Contents

1.1 Fabrication procedure of the bilayer structure.

The photograph of the fabrication procedure was shown in Figure S1, which involves scrape-coating process for the fabrication of the upper GNPs-PDMS layer and spin-coating for the PDMS layer with microstructures. The GNPs concentration plays an important role due to its effects on the absorption of nIR light and the adjustment of the thermal expansion coefficient, as Figure S2 shows.

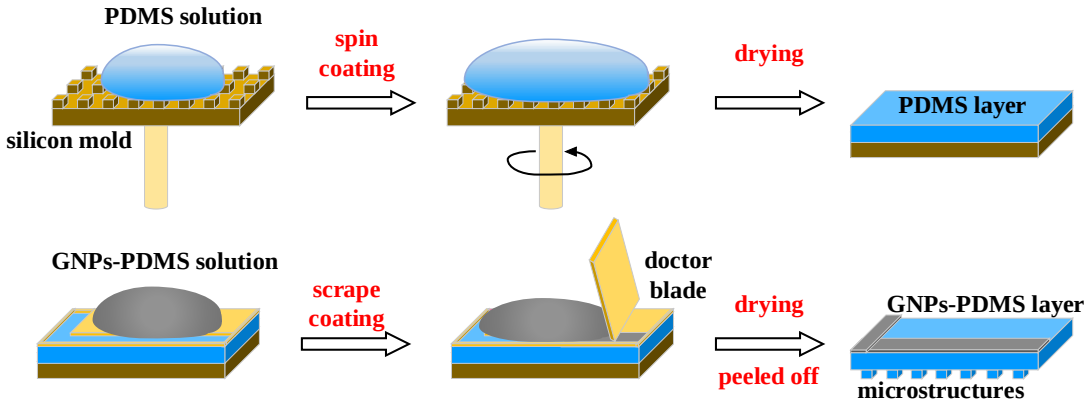

Figure S1. Fabrication scheme of the bilayer structure.

1.2 Effects of graphene concentration on the coefficients of thermal expansion (CTE) and Young's modulus (E).

As Figure S2a shows, the CTE of the GNPs-PDMS layer gradually decreases from 310×10^{-6} m m^{-1} K^{-1} to 163×10^{-6} m m^{-1} K^{-1} as the concentration of GNPs increases to 5%. The Young's modulus E ranged from 0.38MPa to 0.93MPa with the augment of the GNPs weight concentration from 2% to 8%, shows in Figure S2b.

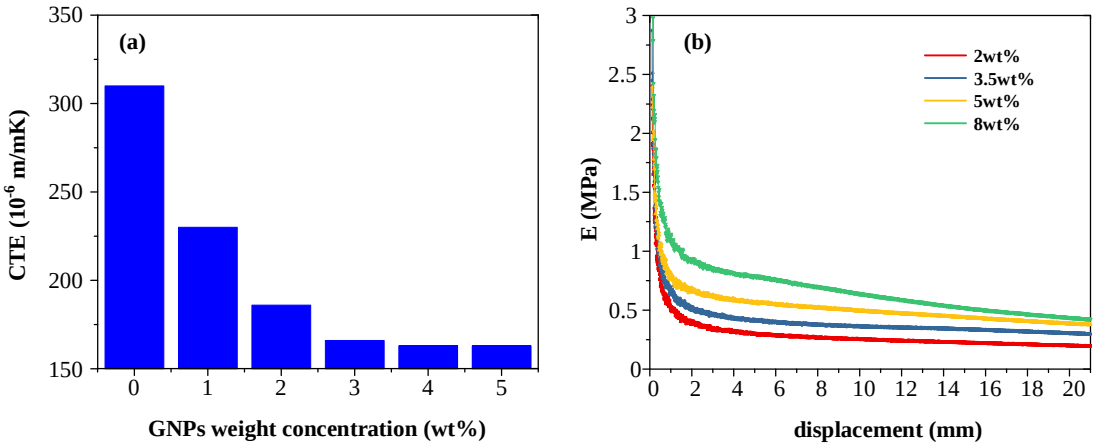

Figure S2. (a) CTE with various GNPs weight concentrations at 25℃. (b) E with various GNPs weight concentrations.

1.3 Swimming mechanism of the soft robot boat.

The deflection of the soft robot boat is similar to the tail swinging of the fish, which based on body and/or caudal fin (BCF) propulsion mechanism, as Figure S3a shows. When the nIR light irradiates the boat tail, the boat will deflect upwards and results in a force disequilibrium, the deflection of the boat tail could generate a propulsion force for the robot to swimming forward, as Figure S3b shows. BCF-based swimming mechanisms have been widely investigated in other bionic fish.[36, S1]

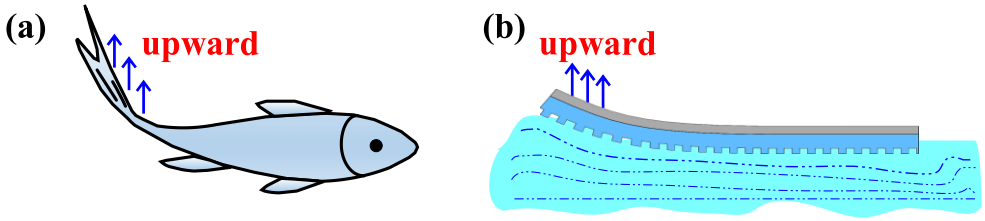

Figure S3. Diagram to demonstrate the swimming mechanism of the soft robot boat. (a) Tail swinging of the fish. (b) Deflection of the soft robot boat.

Supporting reference：

(S1) Wang, Z.; Wang, Y.; Li, J.; Hang, G. A micro biomimetic manta ray robot fish actuated by SMA, *IEEE Int. Conf. Rob. Biomimetics*, **2010**.

1.4 Derivation of robotics loading capacity and calculation details of energy transitions.

(1) Derivation of robotics loading capacity.

According to Young-Laplace equation, the pressure difference ΔP across the solid/liquid/gas interface on a given point, can be written as eq S1.

$$\Delta p = \rho g z = \gamma \frac{z''}{\sqrt{(1+z'^2)^3}} \tag{S1}$$

Where equation $z = h(x)$ is the description of the water/air interface profile, the boundary conditions for $h(x)$ can be written as eqs S2 and S3.

$$\left.\frac{\mathrm{d}z}{\mathrm{d}x}\right|_{x=x_0} = \tan(CA+\varphi) \tag{S2}$$

$$z(\infty) = 0 \tag{S3}$$

As Figure 2 shows, the maximum loading capacity of the soft robot boat is determined by the buoyant force and the weight of floating system before the liquid-boat surface breaks, then $z_{\min}$ can be calculated as eq S4.

$$z_{\min} = \left(1 - \frac{1}{\sqrt{1+\tan^2(CA+\varphi)}}\right)\frac{\gamma}{\rho g}\frac{1}{R(1-\cos\varphi)} - \frac{1}{2}R(1-\cos\varphi) < 0 \tag{S4}$$

Thus the loading capacity can be derived as eq 1.

$$LC+mass=L^2\left|\left(1-\frac{1}{\sqrt{1+\tan^2\left(CA+\varphi\right)}}\right)0.0735\frac{1}{R(1-\cos\varphi)}-\frac{1}{2}R(1-\cos\varphi)\right| \quad (1)$$

Table S1. Derivation of robotics loading capacity and process parameters

Parameters	Notation	Parameters	Notation
surface tension force	F_γ	loading capacity	*LC+mass*
buoyancy force	F_b	density of liquid	ρ
solid-liquid boundary line	$L_{s\text{-}l}$	ridge width	a
air-liquid boundary at A	$L_{a\text{-}l}$	groove width	b
three-phase junction	A(x_0,z_0)	ridge height	h

(2) Detailed information of energy transitions.

$$G_x=\left(1-\cos\theta_c^x\right)^{\frac{2}{3}}\left(2+\cos\theta_c^x\right)^{\frac{1}{3}}\times\sqrt[3]{9\pi}V^{\frac{2}{3}}\gamma \quad (S5)$$

Where θ_c^x is the apparent contact angle of the drop at different state, *x* represents Wenzel or Cassie, *V* is the droplet volume, γ is the liquid–vapor interfacial tension.

$$G_g^x=\left(LC+mass\right)gR_x(1+\cos\theta_c^x) \quad (S6)$$

Where R_x is the curvature radius of droplet at Wenzel or Cassie state.

$$G_C-G_{\max}=(r-1)\cos\theta_c^x\gamma A_c \quad (S7)$$

Where *r* is the roughness ratio, A_c is the solid-liquid contact area projected on the horizontal plane at Cassie state.